

Feasibility and reliability of various morphologic features on magnetic resonance imaging for iliotibial band friction syndrome

Jin Kyem Kim¹, Taeho Kim¹, Hong Seon Lee¹, and Dong Kyu Kim^{1,2}

¹Department of Radiology, The Armed Forces Capital Hospital, Seongnam, Korea

²Department of Radiology, Severance Hospital, Research Institute of Radiological Science, Yonsei University College of Medicine, Seoul, Korea

ABSTRACT

Background: To evaluate the feasibility, inter-reader reliability, and intra-reader reliability for various morphological features reported to be related to iliotibial band friction syndrome (ITBFS) on knee magnetic resonance imaging (MRI).

Methods: A total of 145 patients with a clinical diagnosis and knee MRI findings consistent with ITBFS were included in the “study group” and 232 patients without knee pathology on both physical examination and MRI were included in the “control group”. Various morphologic features on knee MRI were assessed including the patella shape, patella height, lateral epicondyle anterior-posterior (AP) width, lateral epicondyle height, ITB diameter (ITB-d), and ITB area (ITB-a).

Results: Patients in the study group had significantly higher lateral epicondyle height (13.9 mm vs. 12.92 mm, $P = 0.003$), ITB-d (2.9 mm vs. 2.0 mm, $P = 0.022$), and ITB-a (38.5 mm² vs. 23.8 mm², $P < 0.001$) than the control group. ITB-a showed higher area under the curve index (0.849 with 74.1% sensitivity and 72.4% specificity at a 30.3 mm² cutoff) than ITB-d (0.710 with 70.8% sensitivity and 61.2% specificity at 2.4 mm cutoff) and lateral epicondyle height (0.776 with 72.4% sensitivity and 67.8% specificity at 13.4 mm cutoff). However, only the inter-reader agreement for ITB-a (intraclass correlation coefficient = 0.65) was moderate, while the agreements for other morphologic features were good or excellent.

Conclusions: Lateral epicondyle height seems to be a reliable and feasible morphologic feature for diagnosis of ITBFS.

Keywords: Feasibility Studies; Femur; Friction; Iliotibial Band Syndrome; Knee Joint; Magnetic Resonance Imaging; Observer Variation; Patella.

INTRODUCTION

Iliotibial band friction syndrome (ITBFS), commonly seen in young individuals who engage in physical activi-

ties such as running, cycling, or weightlifting, is one of the common causes of lateral knee pain. ITBFS is an overuse injury and is thought to be caused by inflammation of distal part of the ITB due to the repetitive friction and

Received December 2, 2022; Revised December 27, 2022; Accepted January 16, 2023

Handling Editor: Young Hoon Kim

Correspondence: Dong Kyu Kim

Department of Radiology, Severance Hospital, Research Institute of Radiological Science, Yonsei University College of Medicine, 50-1 Yonsei-ro, Seodaemun-gu, Seoul 03722, Korea

Tel: +82-2-2228-7400, Fax: +82-2-393-3035, E-mail: kdk7118@naver.com



This is an Open Access article distributed under the terms of the Creative Commons Attribution Non-Commercial License (<http://creativecommons.org/licenses/by-nc/4.0>), which permits unrestricted non-commercial use, distribution, and reproduction in any medium, provided the original work is properly cited.

abrasion of the ITB across the lateral femoral epicondyle [1,2].

ITBFS is typically diagnosed based on the physical examination and patient's history. Local tenderness 1–2 cm superior to the lateral knee joint line and a history of worsening pain during activity are the main complaints [3]. On magnetic resonance imaging (MRI), ITBFS presents increased signal intensity on T2-weighted imaging along both the deep and superficial parts of the iliotibial tract. MRI can also be helpful to exclude other possible causes of lateral knee pain, such as lateral ligament collateral injury or meniscal tear [4,5].

There were many previous studies to evaluate the morphological imaging features on MRI which may be helpful for diagnosis of ITBFS. Previous studies reported that patella alta, type I and III patella according to Wiberg classification, greater lateral epicondyle prominence, increment in the diameter of ITB, and larger cross-sectional area of the ITB were associated with ITBFS and could be imaging features for diagnosing ITBFS [5–9]. However, there was not much published information demonstrating the feasibility, inter-reader reliability, and intra-reader reliability on these various MR imaging features for diagnosis of ITBFS.

We assumed that the feasibility and reliability would differ in the various morphological MR features reported to be related to ITBFS. Therefore, the primary purpose of this study was to evaluate the feasibility of the morphological MR features for diagnosis of ITBFS. Furthermore, the reliability of the morphologic MR features was also assessed based on inter-reader and intra-reader agreements.

MATERIALS AND METHODS

1. Study population

This retrospective study was approved by the Armed Forces Capital Hospital institutional review board (IRB number: 2022-03-003) and requirements for informed consent were waived.

From January 2016 to January 2021, patients who underwent knee MRI due to lateral knee pain were identified. Among them, patients with a clinical diagnosis of ITBFS and knee MRI findings consistent with ITBFS presenting increased signal intensity between the ITB and the lateral femoral condyle on T2-weighted fat saturation (FS) were included in this study (**Fig. 1**). The exclusion criteria were as follows: 1) patients with a history of trau-

ma or intervention, 2) presence of patellar dislocation, genu varus, genu valgus, and leg length discrepancy, and 3) presence of other knee pathologies including meniscal injury, ligament injury, osteoarthritis (\geq Kellgren–Lawrence grade 2), inflammatory arthritis, or a space-occupying lesion. Finally, a total of 151 knee MRI scans with 145 patients (mean age = 39.1 ± 4.2 years) were included in this study as a “study group”. In the same period, patients who complained of subjective lateral knee pain, but had no diagnosed pathology on both physical examination and MRI were included as a “control group”.

2. MRI protocol

MRI examinations were performed by 3.0-T (Discovery MR 750w; GE Healthcare) or 1.5-T (Signa Explorer; GE Healthcare) MR scanners with the unenhanced knee protocol. The standard protocol of 1.5-T MRI consisted of axial T2-weighted FS (repetition time [TR]/echo time [TE] 3,462/38 ms, 3-mm slice thickness), coronal T1-weighted (TR/TE 476/6 ms, 3.5-mm slice thickness) and T2-weighted FS (TR/TE 5,500/63 ms, 3.5-mm slice thickness), and sagittal proton density (PD)-weighted (TR/TE 2,200/40 ms, 3.5-mm slice thickness) and T2-weighted FS (TR/TE 2,627/41 ms, 3.5-mm slice thickness) sequences through the entire knee using a 32-channel body coil. The field of view (FOV) for each sequence was 18×18 cm with a 384×256 matrix. The protocol of 3.0-T MRI consisted of axial T2-weighted FS (TR/TE 3,424/40 ms, 3-mm slice thickness), coronal T1-weighted (TR/TE 728/8 ms, 3.5-mm slice thickness) and T2-weighted FS (TR/TE 4,162/59 ms, 3.5-mm slice thickness), and sagittal PD-weighted (TR/TE 2,156/41 ms, 3.5-mm slice thickness) and T2-weighted FS (TR/TE 4,018/37 ms, 3.5-mm slice thickness)

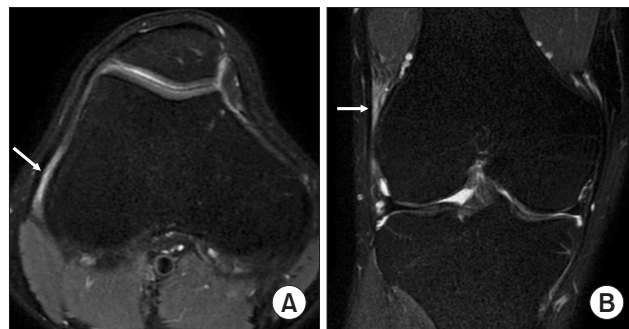


Fig. 1. Magnetic resonance imaging findings of iliotibial band friction syndrome (ITBFS). The white arrows demonstrate the increased signal intensity between the ITB and lateral femoral condyle on axial (A) and coronal (B) T2-weighted fat saturation images.

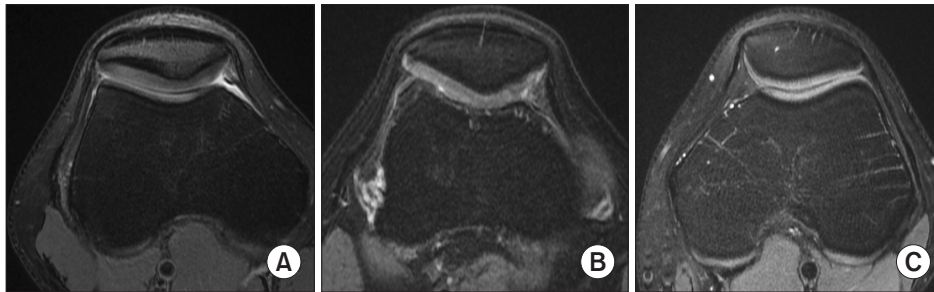


Fig. 2. Assessment of various morphologic findings on knee magnetic resonance imaging. Patella shape was determined on axial T2-weighted fat saturation (FS) images based on Wiberg classification: (A) type I = the medial and lateral facets of the patella are roughly symmetric and concave in shape, (B) type II = lateral facet is slightly longer than medial facet and usually concave shape of lateral facet, (C) type III = medial facet is markedly smaller with more vertical orientation.

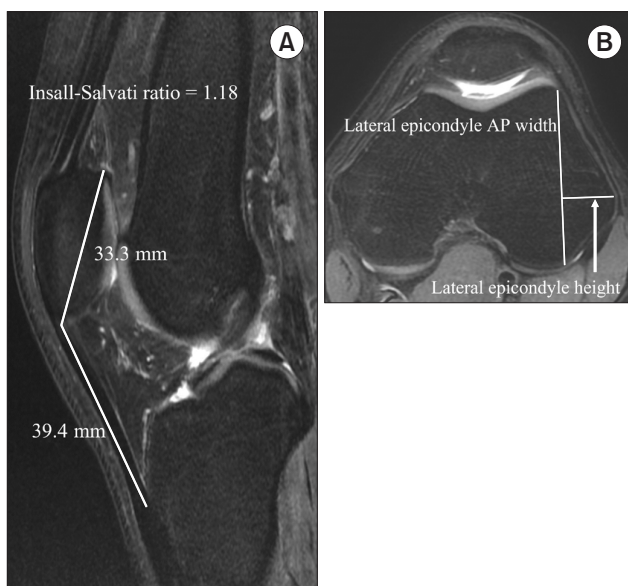


Fig. 3. Assessment of various morphologic findings on knee magnetic resonance imaging. (A) Patella height was determined on sagittal T2-weighted fat saturation (FS) images according to Insall-Salvati ratio. (B) On axial T2-weighted FS images where the lateral epicondyle is the most prominent, lateral epicondyle antero-posterior (AP) width was measured by drawing the line connecting the lateral margin of the anterior and posterior articular surface of the lateral condyle. Then, the lateral epicondyle height was measured by drawing the line perpendicular to the first line toward the most lateral point on the lateral epicondyle (arrow).

sequences using a 23-channel body coil with a FOV of 18 × 18 cm and a 384 × 288 acquisition matrix.

3. Quantitative MR findings and image analysis

Images of knee MRI examination were obtained from the ZeTTA PACS Viewer 2001 (Taeyoung Soft). Various

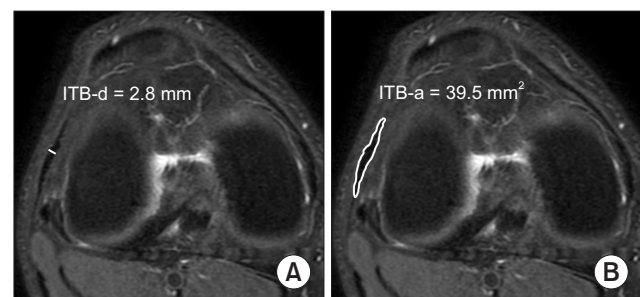


Fig. 4. Assessment of various morphologic findings on knee magnetic resonance imaging. (A) Iliotibial band diameter (ITB-d) was measured in the thickest region at the level of lateral femoral epicondyle on axial T2-weighted fat saturation image. (B) On the same axial image plane, ITB area (ITB-a) was also measured by drawing free-hand region of interests at the thickest ITB.

morphologic features on knee MRI were assessed and calculated as follows: 1) patella shapes were assessed on axial T2-weighted FS image and classified according to Wiberg's classification [10] (**Fig. 2**), 2) the patellar length ratio was measured on sagittal PD-weighted images according to the Insall and Salvati method; then, a ratio lower than 0.8 was determined as patella baja and higher than 1.2 was determined as patella alta [11,12], 3) lateral epicondyle height and anterior-posterior (AP) width was measured on an axial T2-weighted FS image at the point where the lateral epicondyle is the most prominent [6] (**Fig. 3**), 4) ITB diameter (ITB-d) was measured in the thickest region at the level of lateral femoral epicondyle on an axial T2-weighted FS image. On the same axial image plane, the ITB area (ITB-a) was also measured by drawing free-hand region of interests (ROIs) at the thickest ITB [8,9] (**Fig. 4**). All MR images were reviewed by three radiologists with 3, 7, and 8 years of radiology experience, respectively, who were blinded to any clini-

Table 1. Baseline characteristics of study population and comparison between two groups

Variable	Study group (n = 145)	Control group (n = 232)	P value	Total (n = 377)
Age (yr)	39.1 ± 4.2	38.2 ± 7.7	0.711	38.5 ± 6.7
Sex			0.430	
Male	108 (74.5)	181 (78.0)		289 (76.7)
Female	37 (25.5)	51 (22.0)		88 (23.3)
BMI (kg/m ²)	22.5 ± 2.8	22.3 ± 3.0	0.897	22.4 ± 2.9
Affected side of knee			0.821	
Right	79 (54.5)	121 (52.2)		200 (53.1)
Left	60 (41.4)	103 (44.4)		163 (43.2)
Bilateral	6 (4.1)	8 (3.4)		14 (3.7)
Interval periods (days) ^a	38.1 ± 19.0	42.5 ± 11.8	0.523	40.8 ± 12.9
NRS score	3.0 ± 1.6	2.1 ± 1.7	0.138	2.5 ± 1.7

Values are presented as mean ± standard deviation or number (%).

BMI: body mass index, NRS: numeric rating scale.

^aInterval periods: days from the clinical visit to knee magnetic resonance imaging examination.

cal patient information. For assessment of intra-reader reliability, there was at least a 2-week interval period between the first and second interpretations of the knee MRI to minimize recall bias. The feasibility of the various morphologic features for diagnosis of ITBFS was assessed by using the data obtained from the most experienced reader.

4. Clinical information

Clinical information including age, sex, body mass index (BMI), affected knee (right, left, and bilateral), and interval periods from the clinical visit to MRI examination were collected from the electronic medical charts. Subjective pain was evaluated with the use of the numeric rating scale (NRS) at the time of the clinical visit.

5. Statistical analysis

Continuous variables are expressed as mean ± standard deviation. Continuous variables were compared by using independent *t*-tests or one-way analysis of variance, while categorical variables were compared by using χ^2 or Fisher exact tests.

The inter-reader and intra-reader agreements regarding image analysis were evaluated with Cohen's/Fleiss' kappa (κ) statistics and intraclass correlation coefficients (ICCs). The κ values were as follows: κ less than 0.20 indicated poor agreement; κ of 0.21–0.40, fair agreement; κ of 0.41–0.60, moderate agreement; κ of 0.61–0.80, good agreement; and κ greater than 0.81, excellent agreement. ICC results were interpreted according to the following

criteria: poor (ICC < 0.50), moderate (ICC = 0.50–0.74), good (ICC = 0.75–0.90), and excellent (ICC > 0.90) [13,14]. A receiver operating characteristic (ROC) analysis was conducted to assess the performance of various morphologic features for the prediction of ITBFS, based on the values of sensitivity, specificity, and area under curve (AUC). The optimal cut-off value was determined to maximize the sum of sensitivity and specificity.

All statistical analyses were performed with SPSS version 26.0 (IBM Corp.) and MedCalc version 16.2.1 (MedCalc Software). *P* values < 0.05 were considered statistically significant.

RESULTS

1. Study population

There was a total of 145 patients (mean age = 39.1 ± 4.2 years) with 151 knee MRI scans in the study group. The control group consisted of 232 patients (mean age = 38.2 ± 7.7 years) with 240 knee MRI scans. The baseline characteristics of the patients are summarized in **Table 1**. There was no significant difference in age, sex, BMI, affected side of knee, interval periods from the clinical visit to MRI examination, or NRS scores between the two groups.

2. Feasibility of quantitative MR findings for diagnosis of ITBFS

There were significant differences in lateral epicondyle

Table 2. Comparison of morphologic features on knee MRI between two groups

Variable	Study group (n = 151)	Control group (n = 240)	P value	Total (n = 391)
Patella shape			0.552	
Wiberg classification I	49 (32.5)	81 (33.8)		130 (33.2)
Wiberg classification II	85 (56.3)	124 (51.7)		209 (53.5)
Wiberg classification III	17 (11.3)	35 (14.6)		52 (13.3)
Patella height			0.057	
Patella alta	35 (23.2)	33 (13.8)		68 (17.4)
Normal	115 (76.2)	205 (85.4)		320 (81.8)
Patella baja	1 (0.7)	2 (0.8)		3 (0.8)
Lateral epicondyle height (mm)	13.9 ± 6.1	12.9 ± 6.2	0.003	13.3 ± 6.2
Lateral epicondyle AP width (mm)	61.5 ± 7.9	61.6 ± 7.6	0.830	61.6 ± 7.7
ITB-d (mm)	2.9 ± 0.6	2.0 ± 0.7	0.022	2.3 ± 0.8
ITB-a (mm ²)	38.5 ± 8.5	23.8 ± 10.3	< 0.001	29.5 ± 10.8

Values are presented as number (%) or mean ± standard deviation.

MRI: magnetic resonance imaging, AP: anterior-posterior, ITB-d: iliotibial band diameter, ITB-a: iliotibial band area.

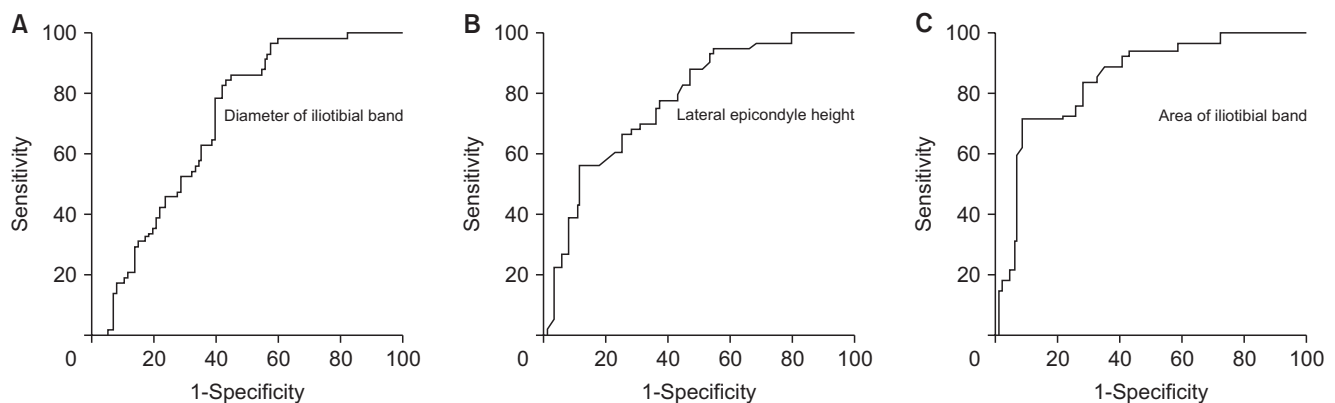


Fig. 5. Receiver operating characteristic analysis to assess the performance of lateral epicondyle height, iliotibial band diameter (ITB-d), and ITB area (ITB-a) for predicting the risk of iliotibial band syndrome. (A) The area under curve (AUC)-index of ITB-d was 0.710 (95% confidence interval [CI]: 0.652–0.768). At a cutoff value of 2.4 mm, the sensitivity and specificity were 70.8% and 61.2%, respectively. (B) The AUC-index of lateral epicondyle height was 0.776 (95% CI: 0.723–0.829). At a cutoff value of 13.4 mm, the sensitivity and specificity were 72.4% and 67.8%, respectively. (C) The AUC-index of ITB-a was 0.849 (95% CI: 0.803–0.894). At a cutoff value of 30.3 mm², the sensitivity and specificity were 74.1% and 72.4%, respectively.

height, ITB-d, and ITB-a between the two groups (**Table 2**). The mean lateral epicondyle height was 13.9 ± 6.1 mm in the study group and 12.9 ± 6.2 mm in the control group ($P = 0.003$). Furthermore, the mean ITB-d (2.9 ± 0.6 mm vs. 2.0 ± 0.7 mm, $P = 0.022$) and ITB-a (38.5 ± 8.5 mm² vs. 23.8 ± 10.3 mm², $P < 0.001$) were also significantly higher in the study group than the control group.

On ROC analysis, the cut-off value of the lateral epicondyle height for predicting ITBFS was 13.4 mm with 72.4% of sensitivity, 67.8% of specificity, and 0.776 (95% confidence interval [CI]: 0.723–0.829) of AUC. The cut-off values of ITB-d and ITB-a were 2.4 mm (sensitivity: 70.8%, specificity: 61.2%, AUC: 0.710 [95% CI: 0.652–0.768])

and 30.3 mm² (sensitivity: 74.1%, specificity: 72.4%, AUC: 0.849 [95% CI: 0.803–0.894]), respectively. Of the three morphologic features associated with ITBFS, ITB-a showed a higher AUC-index (0.849) than that of ITB-d (0.710) and the lateral epicondyle height (0.776) (**Fig. 5**).

3. Inter-reader and intra-reader agreements for morphological MR features

The inter-reader and intra-reader agreements for various morphological MR features are summarized in **Table 3**. Both the inter-reader and intra-reader agreements were excellent for patella shape and patella height. In addition,

Table 3. Inter-reader and intra-reader agreements for various morphologic features

Variable	Inter-reader	Intra-reader		
		Reader A	Reader B	Reader C
Patella shape (κ) ^a	0.81 (0.70–0.86)	0.87 (0.73–0.95)	0.82 (0.72–0.92)	0.84 (0.74–0.93)
Patella height (κ) ^a	0.86 (0.79–0.92)	0.96 (0.90–1.00)	0.90 (0.82–0.96)	0.91 (0.82–0.96)
Lateral epicondyle height	0.84 (0.80–0.88)	0.86 (0.80–0.90)	0.84 (0.76–0.89)	0.88 (0.78–0.95)
Lateral epicondyle AP width	0.82 (0.72–0.88)	0.85 (0.76–0.93)	0.84 (0.74–0.92)	0.82 (0.73–0.90)
ITB-d	0.82 (0.78–0.86)	0.87 (0.73–0.96)	0.83 (0.70–0.91)	0.84 (0.70–0.92)
ITB-a	0.65 (0.56–0.70)	0.76 (0.71–0.81)	0.71 (0.66–0.76)	0.73 (0.69–0.82)

AP: anterior-posterior, ITB-d: iliotibial band diameter, ITB-a: iliotibial band area.

^aPatella shape was classified into type I, II, and III based on the Wiberg classification and patella height was classified into patella alta, patella baja, and normal based on the Insall-Salvati ratio.

both the inter-reader and intra-reader agreements were good for lateral epicondyle height, lateral epicondyle AP width, and ITB-d. However, only the inter-reader agreement for ITB-a (ICC = 0.65) was moderate. The intra-reader agreements for ITB-a were also moderate in two of three readers (ICC = 0.71 in reader B; ICC = 0.73 in reader C).

DISCUSSION

The most important finding of the present study was that ITB-d, ITB-a, and lateral epicondyle height were the morphological features associated with ITBFS. On feasibility assessment, ITB-a (AUC = 0.849) and lateral epicondyle height (AUC = 0.776) showed higher AUC-indexes than ITB-d (AUC = 0.710). However, on reliability assessment, both the inter-reader and intra-reader agreements were lower in ITB-a than lateral epicondyle height and ITB-d. Therefore, considering both feasibility and reliability, lateral epicondyle height could be an accurate morphologic parameter for diagnosis of ITBFS.

ITBFS is one of the most common overuse injuries in the knee joint which occurs due to mechanical repetitive friction of the ITB across the lateral femoral epicondyle. The cumulative effect of repetitive friction may cause an inflammation within the ITB, the periosteum of the lateral femoral epicondyle, and underlying bursa, which eventually results in lateral knee pain [15,16]. However, there are several other diseases which can also cause lateral knee pain including meniscal tear, ligament tear, or *etc.* Therefore, accurate diagnosis of ITBFS is important. Previous studies reported that a higher position of patella (patella alta), lateral epicondyle prominence (increment in lateral epicondyle height), thick ITB, and larger ITB-a were the morphological features associated with ITBFS

[6–9]. However, these are subjectively measured values and there are not many studies on their reliability. Therefore, the inter-reader and intra-reader reliability as well as the feasibility of these various morphological features on knee MRI were assessed in the present retrospective study.

In this study, lateral epicondyle prominence, thick ITB-d, and larger ITB-a were found to be significantly associated factors with ITBFS. This is in line with the results of the previous studies reporting that patients with ITBFS had higher ITB thickness, ITB-a, and lateral epicondyle height than those without ITBFS [6,8,9]. There was still controversy as to whether the thick ITB caused symptoms or the misuse injury caused the ITB-d to increase [8,17]. However, regardless of which assumption is correct, it was found that the increase of ITB-d was associated with ITBFS. Since the diameter of the ITB increases due to hypertrophy of the ITB, it also can be hypothesized that the area of the ITB may also increase in patients with ITBFS. In addition, lateral epicondyle prominence may have a cumulative effect to other causes of ITBFS including ITB tightness or hip abductor weakness [18,19].

Some previous studies reported that a higher position of the patella was associated with ITBFS [5,7]. However, in the present study, there was no significant difference in patella height ($P = 0.057$) between the study group and the control group. However, though there was no significant difference, the proportion of patella alta was higher in the study group than the control group (23.2% vs. 13.8%). The result could change depending on the sample size; thus, the presence of patella alta maybe useful as an auxiliary means to diagnose ITBFS. Further study is needed to elucidate the relationship between patella height and ITBFS.

For quantitative measurement of a hypertrophied ITB, there are two main methods: measurement of the ITB-d

or the ITB-a. It may be easy, rapid, and relatively constant to measure the ITB-d. However, measurement mistakes could occur when there is an asymmetrical partial tear or thickening of the ITB. In contrast to the measurement of diameter (ITB-d), ITB-a can reduce the risk of such measurement mistakes because it measures a cross-sectional area of the whole ITB. However, ITB-a measured by manual drawing of ROIs could be inconsistent and inaccurate. On ROC analysis, the AUC-index of ITB-a showed a higher AUC-index (0.849 with 74.1% sensitivity and 72.4% specificity) than that of ITB-d (0.710 with 70.8% sensitivity and 61.2% specificity) and lateral epicondyle height (0.776 with 72.4% sensitivity and 67.8% specificity). However, the inter-reader reliability of ITB-a (ICC = 0.65, moderate agreement) was inferior to that of lateral epicondyle height (ICC = 0.84, good agreement) and ITB-d (ICC = 0.82, good agreement). All three readers' intra-reader agreements of ITB-a (ICC = 0.76, 0.71, and 0.73) were also inferior to those of lateral epicondyle height (ICC = 0.86, 0.84, and 0.88) and ITB-d (ICC = 0.87, 0.83, and 0.84). Therefore, considering not only AUC-index but also inter-reader/intra-reader reliability, lateral epicondyle prominence seems to be a reliable and feasible morphologic finding associated with ITBFS. The ITB-a was evaluated based on free-drawing ROIs manually at selected sites. Manual drawing of ROIs can be inaccurate due to operator bias and may differ depending on the radiologists' experience and career. This is a limitation of the research conducted using the free-drawing ROI method. Therefore, future study with a software system which can automatically detect the ITB and calculate the area of the ITB is needed to elucidate if ITB-a can be an imaging feature with high reliability and feasibility for diagnosis of ITBFS.

There are some limitations in this study. First, it had a retrospective design; so, it may have involved selection bias. Second, this was a single-center study. Therefore, future research in different racial groups with larger sample sizes may provide further insight into the usefulness of the various morphologic features for ITBFS, since genetics and/or environmental factors may play a role in determining the features of the patella, lateral femoral epicondyle, and ITB thickness. Third, patella height, ITB-d, and ITB-a could be changed at different knee flexion angles during the MRI examination. However, knee MRI scanning was performed with knee extension in each patient at the authors' hospital and knee extension would be maintained during MRI examination considering the knee position. Fourth, in this study, the control group consisted of 232 patients who had no diagnosed pathology

on both physical examination and knee MRI. To provide the statistically significant morphologic features and validate the cutoff values of each feature in an ITBFS group compared with healthy individuals, future study with comparable control groups constructed by using a propensity score matching method may be necessary.

In conclusion, lateral epicondyle prominence, thick ITB-d, and larger ITB-a were the morphologic features significantly associated with ITBFS. Considering inter-reader and intra-reader reliability, lateral epicondyle prominence with a 13.4 mm cutoff value for lateral epicondyle height seems to be a reliable and feasible morphologic feature for diagnosis of ITBFS. Therefore, it can be helpful for physicians and radiologists to diagnose the ITBFS. Further study with a software system automatically detecting and measuring ITB-a may provide further insight into the reliability of ITB-a for diagnosis of ITBFS.

DATA AVAILABILITY

The datasets supporting the findings of this study are not publicly available because the organization's IRB restricts access to patient data due to concerns over the risk of inadvertent disclosure of personal health information. However, all relevant data are within the manuscript.

CONFLICT OF INTEREST

No potential conflict of interest relevant to this article was reported.

FUNDING

No funding to declare.

AUTHOR CONTRIBUTIONS

Jin Kyem Kim: Writing/manuscript preparation; Taeho Kim: Data curation; Hong Seon Lee: Investigation; Dong Kyu Kim: Study conception.

ORCID

Jin Kyem Kim, <https://orcid.org/0000-0002-3710-444X>
Taeho Kim, <https://orcid.org/0000-0003-3709-2044>

Hong Seon Lee, <https://orcid.org/0000-0003-2427-2783>
 Dong Kyu Kim, <https://orcid.org/0000-0001-7322-2550>

REFERENCES

1. Orava S. Iliotibial tract friction syndrome in athletes—an uncommon exertion syndrome on the lateral side of the knee. *Br J Sports Med* 1978; 12: 69-73.
2. Khaund R, Flynn SH. Iliotibial band syndrome: a common source of knee pain. *Am Fam Physician* 2005; 71: 1545-50.
3. Hong JH, Kim JS. Diagnosis of iliotibial band friction syndrome and ultrasound guided steroid injection. *Korean J Pain* 2013; 26: 387-91.
4. Flato R, Passanante GJ, Skalski MR, Patel DB, White EA, Matcuk GR Jr. The iliotibial tract: imaging, anatomy, injuries, and other pathology. *Skeletal Radiol* 2017; 46: 605-22.
5. Bankaoglu M, Mahmutoglu AS, Celebi I, Eren OT, Erturk SM, Kilic E, et al. Association of iliotibial band friction syndrome with patellar height and facets variations: a magnetic resonance imaging study. *Iran J Radiol* 2018; 15: e63459.
6. Everhart JS, Kirven JC, Higgins J, Hair A, Chaudhari AA, Flanigan DC. The relationship between lateral epicondyle morphology and iliotibial band friction syndrome: a matched case-control study. *Knee* 2019; 26: 1198-203. Erratum in: *Knee* 2020; 27: 1291.
7. Li J, Sheng B, Qiu L, Yu F, Lv FJ, Lv FR, et al. A quantitative MRI investigation of the association between iliotibial band syndrome and patellofemoral malalignment. *Quant Imaging Med Surg* 2021; 11: 3209-18.
8. Agridag Ucpinar B, Bankaoglu M, Eren OT, Erturk SM. Measurement of iliotibial band diameter in iliotibial band friction syndrome and comparison with an asymptomatic population. *Acta Radiol* 2021; 62: 1188-92.
9. Park J, Cho HR, Kang KN, Choi KW, Choi YS, Jeong HW, et al. The role of the iliotibial band cross-sectional area as a morphological parameter of the iliotibial band friction syndrome: a retrospective pilot study. *Korean J Pain* 2021; 34: 229-33.
10. Wibeeg G. Roentgenographs and anatomic studies on the femoropatellar joint: with special reference to chondromalacia patellae. *Acta Orthop Scand* 1941; 12: 319-410.
11. Insall J, Salvati E. Patella position in the normal knee joint. *Radiology* 1971; 101: 101-4.
12. Shabshin N, Schweitzer ME, Morrison WB, Parker L. MRI criteria for patella alta and baja. *Skeletal Radiol* 2004; 33: 445-50.
13. McHugh ML. Interrater reliability: the kappa statistic. *Biochem Med (Zagreb)* 2012; 22: 276-82.
14. Bland JM, Altman DG. Statistical methods for assessing agreement between two methods of clinical measurement. *Lancet* 1986; 1: 307-10.
15. Walbron P, Jacquot A, Geoffroy JM, Sirveaux F, Molé D. Iliotibial band friction syndrome: an original technique of digastric release of the iliotibial band from Gerdy's tubercle. *Orthop Traumatol Surg Res* 2018; 104: 1209-13.
16. Foch E, Milner CE. Influence of previous iliotibial band syndrome on coordination patterns and coordination variability in female runners. *J Appl Biomech* 2019; 35: 305-11.
17. Ekman EF, Pope T, Martin DF, Curl WW. Magnetic resonance imaging of iliotibial band syndrome. *Am J Sports Med* 1994; 22: 851-4.
18. Fredericson M, Cookingham CL, Chaudhari AM, Dowdell BC, Oestreicher N, Sahrmann SA. Hip abductor weakness in distance runners with iliotibial band syndrome. *Clin J Sport Med* 2000; 10: 169-75.
19. Messier SP, Edwards DG, Martin DF, Lowery RB, Cannon DW, James MK, et al. Etiology of iliotibial band friction syndrome in distance runners. *Med Sci Sports Exerc* 1995; 27: 951-60.